



# A highly active nano-micro hybrid derived from Cu-bridged $\text{TiO}_2$ /porphyrin for enhanced photocatalytic hydrogen production

Xingyu Guo<sup>a</sup>, Xiangqing Li<sup>a,\*</sup>, Lixia Qin<sup>a</sup>, Shi-Zhao Kang<sup>a</sup>, Guodong Li<sup>b</sup>

<sup>a</sup> School of Chemical and Environmental Engineering, Center of Graphene Research, Shanghai Institute of Technology, 100 Haizhu Road, Shanghai, 201418, China

<sup>b</sup> State Key Laboratory of Inorganic Synthesis and Preparative Chemistry, College of Chemistry, Jilin University, Changchun, 130012, China



## ARTICLE INFO

### Keywords:

$\text{TiO}_2$  nano-micro hybrid  
Interfacial modification  
Interaction  
Photocatalytic hydrogen production  
Charge separation

## ABSTRACT

Development of photocatalysts with high activity and durability for hydrogen generation is extremely desired but still remains a great challenge currently. With Cu nanoparticles (Cu NPs) as a linker between  $\text{TiO}_2$  microsphere ( $\text{TiO}_2$  MS) and 5, 10, 15, 20-meso-tetra(4-carboxyphenyl)porphyrin (TCPP), a novel nano-micro hybrid ( $\text{TiO}_2$  MS-Cu-TCPP) was prepared via a facile method. By bridging  $\text{TiO}_2$  MS and TCPP with Cu NPs, the absorption and the electron transfer of  $\text{TiO}_2$  MS were greatly improved. When the  $\text{TiO}_2$  MS-Cu-TCPP was employed as the photocatalyst for hydrogen evolution, it exhibited higher activity and stability than those of the  $\text{TiO}_2$  MS, the  $\text{TiO}_2$  MS-Cu and the  $\text{TiO}_2$  MS-TCPP,  $\text{TiO}_2$  MS-Cu-CuTCPP and  $\text{TiO}_2$  MS-TCPP-Cu. The photocatalytic activity was enhanced for about 6 times with respect to that of the pristine  $\text{TiO}_2$  MS. The excellent performance for the nano-micro hybrid can be attributed to wide light absorption, more reactive sites, and facilitated interfacial electron transfer owing to the strong interaction between  $\text{TiO}_2$  and TCPP with Cu NPs as the linker and cocatalyst. Subsequently, a high and stable photocatalytic activity over the  $\text{TiO}_2$  MS-Cu-TCPP nano-micro hybrid was achieved, demonstrating the importance of interfacial modification to a semiconductor photocatalyst. This result gives us a new perspective of constructing special structures for efficient light utilization and electron transfer.

## 1. Introduction

Photocatalytic hydrogen production driven by free and sustainable solar energy is considered as one of the promising strategies for resolving global energy and environmental problems, owing to its production with no reliance on fossil fuels and no carbon dioxide emission [1–3]. As a promising candidate photocatalyst,  $\text{TiO}_2$  is used widely because of its low cost, nontoxicity, availability, and stability against the light irradiation [4,5]. It is known that the photocatalytic performance of  $\text{TiO}_2$  has close relationship with its morphology [6].  $\text{TiO}_2$  microsphere ( $\text{TiO}_2$  MS) with three-dimensional mesoporous architecture can enhance light-scattering and light-harvesting, which shows excellent performance in photoelectric application [7]. Unfortunately, with pure  $\text{TiO}_2$  as the photocatalyst, low visible adsorption due to its wide band gap, and quick electron-hole recombination extremely limit its photocatalytic performance for hydrogen evolution. Therefore, how to enhance its photocatalytic activity is still a significant issue. As frequently reported, the structural design of a photocatalyst plays a key role in determining the photocatalytic performance for hydrogen production, which requires high light absorption, fast electron transfer, and good stability [8,9]. Many approaches have been proposed, and

much effort has also been made to develop the novel photocatalysts with special structure to satisfy these requirements.

With high visible light absorption and straightforward solar energy-to-chemical conversion facility, porphyrins are regarded as excellent photoactive materials [10,11]. Sharon et al. reported that a visible photoactive porphyrin/ $\text{TiO}_2$  composite prepared via adsorption at room temperature exhibits a good photocatalytic degradation activity for pharmaceuticals [12]. Georgios et al. reported a photocatalytic system with Sn-porphyrin as the photosensitizer, and the target complex exhibited high photocatalytic activity [13]. In these systems, the introduction of porphyrins can only enhance the light absorption of the photocatalysts, and the separation and transfer of photo-generated charges has been hardly affected.

Generally, fast charge carrier recombination for  $\text{TiO}_2$  can be effectively inhibited by loading noble metal (Au, Ag, and Pt) [14]. Alternatively, loading with transition metals such as Cu, Fe, Co, and Ni has recently turned out to be a cheaper and efficient option [15]. Several reports have also revealed the effectiveness of Cu cocatalyst in photocatalysis over noble metals [16]. Therefore, by constructing the specific structure with Cu and porphyrin, it will be very advantageous for improving the activity of  $\text{TiO}_2$ -based photocatalysts. In our previous

\* Corresponding author.

E-mail address: [xqli@sit.edu.cn](mailto:xqli@sit.edu.cn) (X. Li).

reports [17,18], it was found that the composites with high light absorption and electron transfer can be achieved by linking porphyrins onto the  $\text{Cu}_2\text{O}$  by means of hydrogen bond interaction and coordination interaction, which are very advantageous to improve the photocatalytic activity of  $\text{Cu}_2\text{O}$ . However, the problems, especially the difficult recovery due to its small size and the instability in strong acid/base, need to be solved. Therefore, it is still a challenge to construct special structures for stable, easily recovered, and highly efficient photocatalytic hydrogen production without loading additional cocatalyst.  $\text{TiO}_2$  MS with three-dimensional mesoporous architecture is more stable in acidic or basic environment, and is easier to be recovered due to its larger size, which are important factors in catalysis research as well as for practical application.

Herein, a novel  $\text{TiO}_2$  microsphere/meso-tetra(4-carboxyphenyl) porphyrin (TCPP) nano-micro hybrid linked by metallic Cu is facilely prepared by means of coordination interaction and electrostatic interaction. The as-prepared  $\text{TiO}_2$  MS hybrid possesses unique hierarchical structure. The assembly mechanism of the hybrid is explored. Moreover, photocatalytic hydrogen production over the hybrid is investigated in detail. Fluorescence, photoelectronic response and electrochemical impedance are performed to elucidate the detailed mechanism of electron transfer.

## 2. Experimental

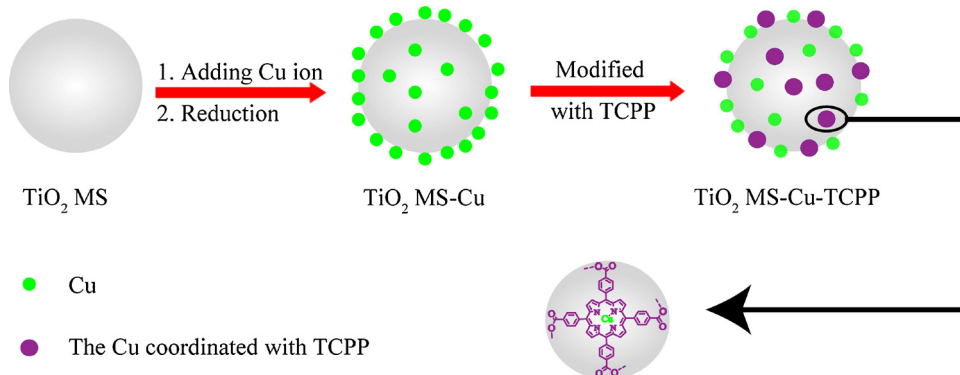
### 2.1. Materials

Polyethylene glycol 200 (PEG 200) and  $\text{Cu}(\text{NO}_3)_2 \cdot 3\text{H}_2\text{O}$  were purchased from Sinopharm Chemical Reagent Company. Hydrazine hydrate, urea and ethanol were purchased from Shanghai Taitan Scientific Co., Ltd.  $\text{TiCl}_3$  hydrochloric acid solution was purchased from Aladdin Industrial Co. Trisodium citrate dehydrate ( $\text{Na}_3\text{C}_6\text{H}_5\text{O}_7 \cdot 2\text{H}_2\text{O}$ ) was purchased from Shanghai Chemical Reagent Company. Meso-tetra(4-carboxyphenyl) porphyrin (TCPP) was purchased from J&K Scientific Ltd. All chemicals used were analytical grade reagents without further purification.

### 2.2. Synthesis of the $\text{TiO}_2$ MS-Cu-TCPP hybrid

Firstly,  $\text{TiO}_2$  MS were synthesized via a modified solvothermal process [19]. In a typical experimental procedure, 12 mL PEG 200 and 2.4 g urea were dissolved in 30 mL ethanol, and the solution was further magnetically stirred until it became clarified. Then, 12 mL  $\text{TiCl}_3$  hydrochloric acid solution was added, and the mixed solution was transferred to a 100 mL Teflon-lined autoclave immediately. The autoclave was sealed and maintained at 150 °C for 12 h. The solid was collected and washed with ethanol and distilled water, respectively, and dried at 60 °C.

$\text{TiO}_2$  MS-Cu-TCPP hybrid was obtained by the following procedure



**Scheme 1.** Schematic illustration for preparing the  $\text{TiO}_2$  MS-Cu-TCPP hybrid.

### (Scheme 1).

In a typical synthesis, 120 mg  $\text{Cu}(\text{NO}_3)_2 \cdot 3\text{H}_2\text{O}$  was added into 150 mL water, and then 300 mg  $\text{TiO}_2$  MS was added. After being stirred for 40 min, 50 mL of 1.47 mol  $\text{L}^{-1}$  sodium citrate solution was added into the mixture, and continuously stirred until the color of the solution did not change any more. Then, 10 mL of hydrazine hydrate was added and slightly stirred overnight. Finally, the precipitate ( $\text{TiO}_2$  MS-Cu) was collected by centrifugation, and washed and dried at 60 °C.

100 mg of  $\text{TiO}_2$  MS-Cu was added into 50 mL of  $7.6 \times 10^{-6}$  mol  $\text{L}^{-1}$  TCPP methanol solution, and stirred for 8 h at room temperature. The solid was collected, and dried in a vacuum oven at 60 °C. Subsequently,  $\text{TiO}_2$  MS-Cu-TCPP nanohybrid was obtained by hydrogen bond interaction coming from carboxylic groups of TCPP with the hydroxyl groups on  $\text{TiO}_2$  MS (confirmed by the followed UV-vis spectra and FTIR spectra), and coordination interaction between the Cu on the  $\text{TiO}_2$  MS and the N atoms located at the center of the TCPP macrocycle (evidenced by the followed UV-vis spectra, FTIR spectra and XPS spectra), just like that shown in Scheme 1. The content of TCPP in the hybrid was about 0.25 wt %. For comparison,  $\text{TiO}_2$  MS-TCPP,  $\text{TiO}_2$  MS-TCPP-Cu and  $\text{TiO}_2$  MS-Cu-CuTCPP were also synthesized by similar procedure.

### 2.3. Characterizations

Powder XRD diffraction was carried out using a Bruker D8 Advance X-ray diffractometer (Germany). The transmission electron microscope images were taken using a JEOL JEM-1400 microscope (Japan). The element maps were taken with a Hitachi S-4800 cold field emission scanning electron microscope operated at an accelerating voltage of 20 kV (Japan). The surface morphology of the samples was observed by S-3400 N Hitachi High Technologies scanning electron microscopy (SEM, Japan). UV-vis absorption spectra were recorded with a UV-3900 spectrophotometer (Japan). Fourier transform infrared spectra (FTIR) were measured using a Nicolet 6700 FTIR spectrometer (USA). X-ray photoelectron spectroscopy analyses were performed using a Thermo ESCALAB 250X-RAY photoelectron spectrometer with an Al (K $\alpha$ ) X-ray resources (USA).

### 2.4. Photoelectrochemical measurements

The photoelectrochemical performance of all samples was measured by a CHI660E electrochemical system using a three-electrode cell (Shanghai Chenhua Instruments, China). An Ag/AgCl electrode was used as the reference electrode, a platinum wire as the counter electrode, and fluorine-tin oxide (FTO) glasses coated with the sample were utilized as working electrodes. Before being coated the sample, the FTO glasses were ultrasonically cleaned with double distilled water, acetone, chloroform and ethanol for 20 min, respectively, and then dried in the atmosphere. The working electrode was prepared via dip-coating and subsequently natural drying. In brief, 2 mg of sample was dispersed into

4 mL of water. After that, the mixture was dip-coated onto the FTO glass ( $1 \times 1.5 \text{ cm}^2$ ), and then was dried in the atmosphere. A 150 W Xenon lamp was used as the light source. The distance between the lamp and the FTO electrode was 7 cm. The electrolyte solution was  $0.5 \text{ mol L}^{-1}$  of  $\text{Na}_2\text{SO}_4$  aqueous solution, and bias voltage was set in 0.1 V. All measurements were carried out at room temperature.

### 2.5. Measurement of photocatalytic hydrogen evolution

The photocatalytic activity for hydrogen evolution over the samples was performed through a CEL-SP2 N water splitting system (Zhongjiao Jinyuan Instruments, China). For photocatalytic hydrogen evolution, 10 mg of photocatalyst was dispersed by a magnetic stirrer in an up-irradiated photocatalytic reactor containing an aqueous solution of triethanolamine (TEOA) (60 mL, volume ratio of water to TEOA is 5: 1). The reaction cell was connected to a gas circulation system, and the hydrogen evolved was analyzed by an online gas chromatograph (NaX zeolite column, high-purity  $\text{N}_2$  as carrier gas, thermal conductivity detector). The reaction temperature was kept at about  $5.5^\circ\text{C}$  by a circulating water jacket. A 300 W Xe lamp was used as the light source. The gas produced was automatically sampled and analyzed by an online gas chromatography. Before the photocatalytic reaction, the reactor was evacuated by a vacuum pump and flushed by nitrogen for several times to ensure complete removal of oxygen.

## 3. Results and discussion

### 3.1. Material characterization

The  $\text{TiO}_2$  MS-Cu-TCPP nano-micro hybrid was fabricated by means of hydrogen bond interaction and electrostatic interaction with Cu NPs as the linker. **Scheme 1** shows the schematic illustration of the formation of the  $\text{TiO}_2$  MS-Cu-TCPP hybrid. First, the  $\text{TiO}_2$  MS was loaded with Cu NPs by electrostatic interaction and in-situ reduction, and then the  $\text{TiO}_2$  MS-Cu was added into the TCPP solution. After reacted at room temperature, the  $\text{TiO}_2$  MS-Cu-TCPP nano-micro hybrid was obtained, and showed relatively rough surface morphology (Fig. 1). The  $\text{TiO}_2$  MS-Cu-TCPP hybrid was formed owing to the special interaction among  $\text{TiO}_2$ , Cu NPs and TCPP, which will be evidenced by the following Fig. 1–5.

Fig. 1 shows the SEM and TEM images of the samples. As can be

shown in Fig. 1a,  $\text{TiO}_2$  MS with a diameter of  $\sim 3 \mu\text{m}$  are obtained by solvothermal treatment at  $150^\circ\text{C}$  for 12 h, and the spheres are composed of nanocrystallites. After being coated with Cu NPs, the surface of microspheres becomes rough (Fig. 1b and d), which is different from the pure  $\text{TiO}_2$  MS. It indicates the existence of Cu NPs on the  $\text{TiO}_2$  MS. Furthermore, after introducing TCPP onto the Cu NPs coated  $\text{TiO}_2$  MS, no scattered particles are observed outside of the microspheres, and the rough surface becomes relatively smooth. Moreover, the sphere-like morphology remains well. It is indicated that TCPP molecules lay on the microspheres. The morphology could be attributed to the unique loading mode of TCPP molecules on the microspheres, which will be further evidenced by Figs. 3–5. Furthermore, the HRTEM of the hybrid shows (111) face of Cu, (020) and (112) faces of  $\text{CuO}$  on the edge of the microsphere, which indicates that the Cu in the hybrid is mainly in the form of metallic Cu and  $\text{CuO}$ .

To further clarify the component of the  $\text{TiO}_2$  MS-Cu-TCPP, energy-filtered TEM of the hybrid is taken because it can show clearer elemental distribution in the hybrid. Fig. 2 b–f shows the element maps of the hybrid, which are measured according to the image shown in Fig. 2a. It can be seen that there exist Ti, O, Cu, N, C elements in the hybrid, which is consistent with the element composition of the  $\text{TiO}_2$  MS-Cu-TCPP. Moreover, the maps of Ti, O, Cu, N, C shown in Fig. 2b–f, respectively, correspond exactly to the TEM image in Fig. 2a.

The phase and crystallographic structure of the samples were determined by powder X-ray diffraction (XRD). Fig. 3 shows the XRD patterns of  $\text{TiO}_2$  MS,  $\text{TiO}_2$  MS-Cu, and  $\text{TiO}_2$  MS-Cu-TCPP, respectively. The XRD patterns of all products present similar profiles and major peaks are well coincident with standard JCPDS values (anatase-JCPDS No: 21-1272, rutile-JCPDS No: 21-1276). In addition, a new and weak peak at  $2\theta = 42.7^\circ$  is observed at the XRD pattern of the  $\text{TiO}_2$  MS-Cu, which can be assigned to the (111) crystal planes of Cu (JCPDS No: 04-0836). It is demonstrated that the  $\text{Cu}^{2+}$  in the samples has been reduced into metal Cu. The other diffraction peaks of Cu are not found in the Fig. 3, perhaps because of the low content of Cu in the hybrid. In the XRD pattern of the  $\text{TiO}_2$  MS-Cu-TCPP, besides the peaks corresponding to  $\text{TiO}_2$ , the peak (at  $2\theta = 42.7^\circ$ ) attributed to metal Cu in the  $\text{TiO}_2$  MS-Cu is weakened, and a new peak at  $2\theta = 47.5^\circ$  is observed, which corresponds to the crystal facet of (112) crystal planes of  $\text{CuO}$  (JCPDS No: 48-1548). It is deduced that some Cu NPs on the surface of the hybrid could be partially oxidized due to the linking of TCPP on the  $\text{TiO}_2$  MS-Cu.

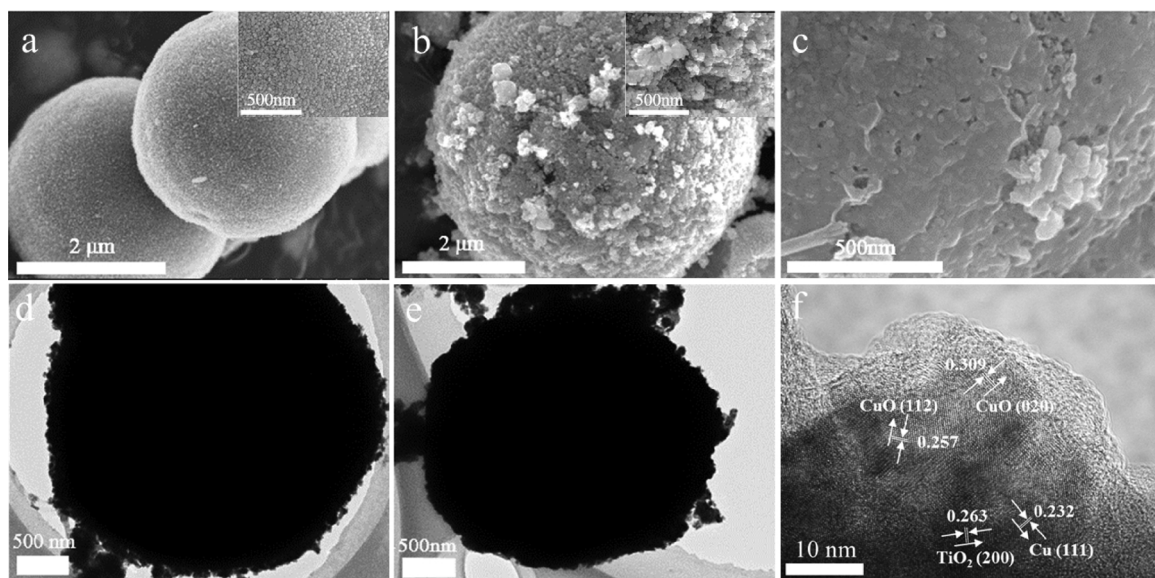


Fig. 1. SEM images of (a)  $\text{TiO}_2$  MS, (b)  $\text{TiO}_2$  MS-Cu, (c)  $\text{TiO}_2$  MS-Cu-TCPP. TEM images of (d)  $\text{TiO}_2$  MS-Cu, (e)  $\text{TiO}_2$  MS-Cu-TCPP and HRTEM image of (f)  $\text{TiO}_2$  MS-Cu-TCPP. The insets were the corresponding enlarged images.

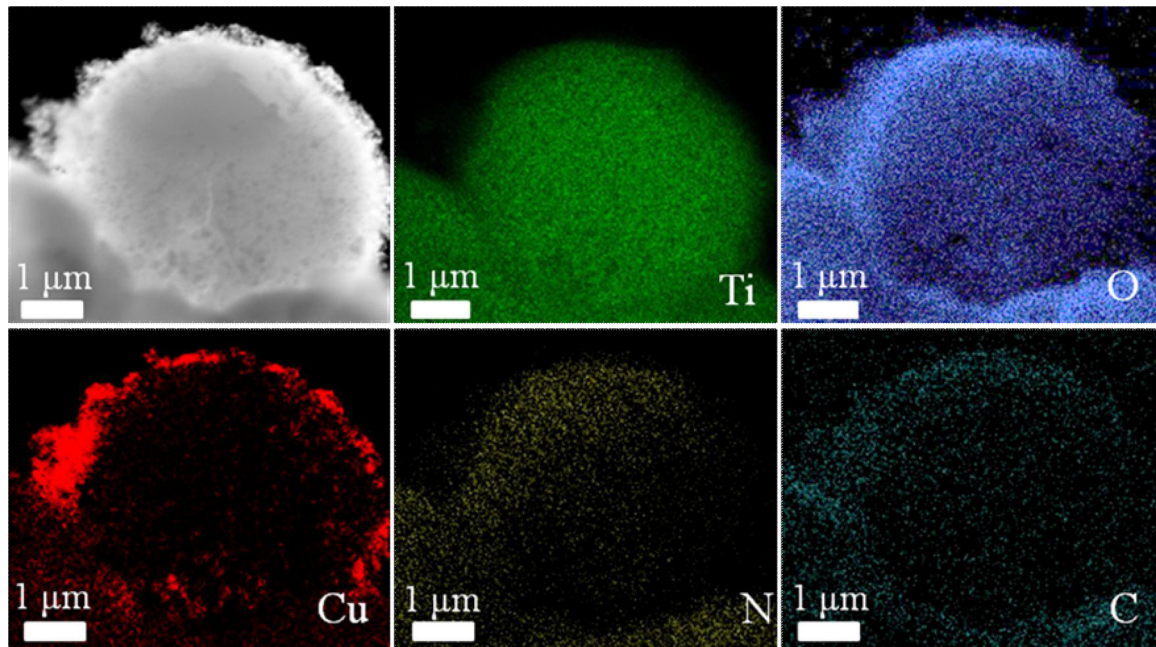


Fig. 2. Energy-filtered TEM images of the  $\text{TiO}_2$  MS-Cu-TCPP. (a) TEM image, (b) Ti map; (c) O map; (d) Cu map; (e) N map and (f) C map.

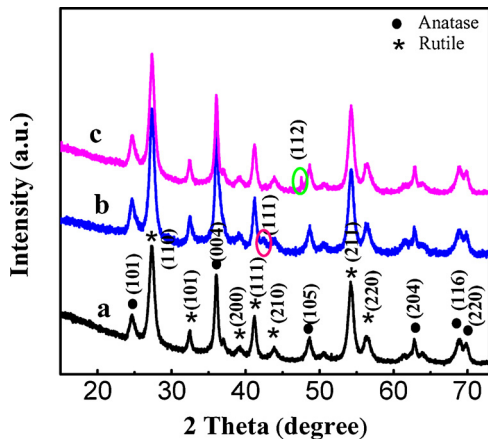


Fig. 3. XRD patterns of (a)  $\text{TiO}_2$  MS, (b)  $\text{TiO}_2$  MS-Cu and (c)  $\text{TiO}_2$  MS-Cu-TCPP.

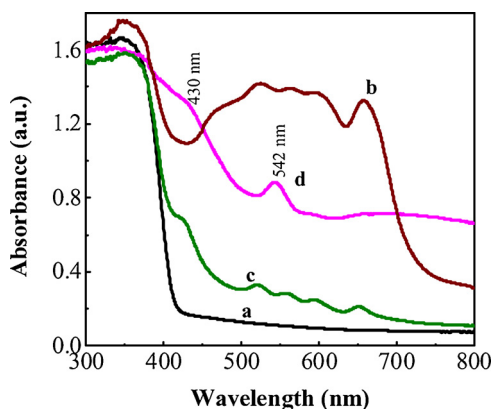


Fig. 4. UV-vis diffuse reflectance absorption spectra of (a)  $\text{TiO}_2$  MS, (b) TCPP, (c)  $\text{TiO}_2$  MS-TCPP, and (d)  $\text{TiO}_2$  MS-Cu-TCPP.

Fig. 4 shows UV-vis diffuse reflectance spectra of the samples, which are recorded in the range of 300–750 nm. Obviously, no absorption is observed above 400 nm for bare  $\text{TiO}_2$  MS. The band edge at

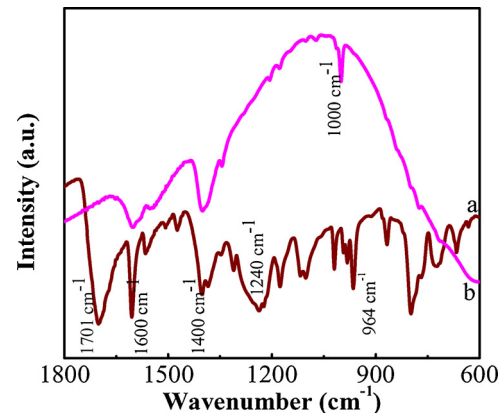


Fig. 5. The FTIR spectra of (a) TCPP and (b)  $\text{TiO}_2$  MS-Cu-TCPP.

about 390 nm indicates a band gap of about 3.1 eV, which is consistent with the direct absorption of the intrinsic band gap of  $\text{TiO}_2$  [20]. In the spectrum of  $\text{TiO}_2$  MS-TCPP (Fig. 4c), the characteristics bands of TCPP can be observed (a Soret band at 423 nm, and four Q bands at 522 nm, 558 nm, 597 nm and 651 nm, respectively). Compared with those of the TCPP, the bands are shifted, which indicate that there exists some interaction between  $\text{TiO}_2$  MS and TCPP. Differently, after introducing Cu NPs between  $\text{TiO}_2$  MS and TCPP, only one Q band is observed, and the Soret band is red-shifted 7 nm, indicating that TCPP had been linked onto the  $\text{TiO}_2$  MS-Cu [21]. According to the spectrum of the  $\text{TiO}_2$  MS-Cu-TCPP, it is deduced that TCPP molecules are combined with the  $\text{TiO}_2$  MS-Cu in the following two ways: hydrogen bond interaction coming from carboxyl groups of TCPP and hydroxyl groups of  $\text{TiO}_2$  MS; and coordination interaction between TCPP macrocycle and the Cu on  $\text{TiO}_2$  MS, just like that shown in Scheme 1. The strong interaction between the  $\text{TiO}_2$  MS-Cu and the TCPP is very profitable to improving electron transfer and photocatalytic activity of the hybrid, which will be further confirmed by the results in Figs. 5–8.

The binding mode of TCPP and  $\text{TiO}_2$  MS-Cu was further confirmed by FTIR (Fig. 5). In Fig. 5, the band at  $964\text{ cm}^{-1}$  is assigned to N–H vibration of the pyrrole ring in the TCPP macrocycle. In addition, some functional groups in TCPP, such as, the C=O stretching vibration band

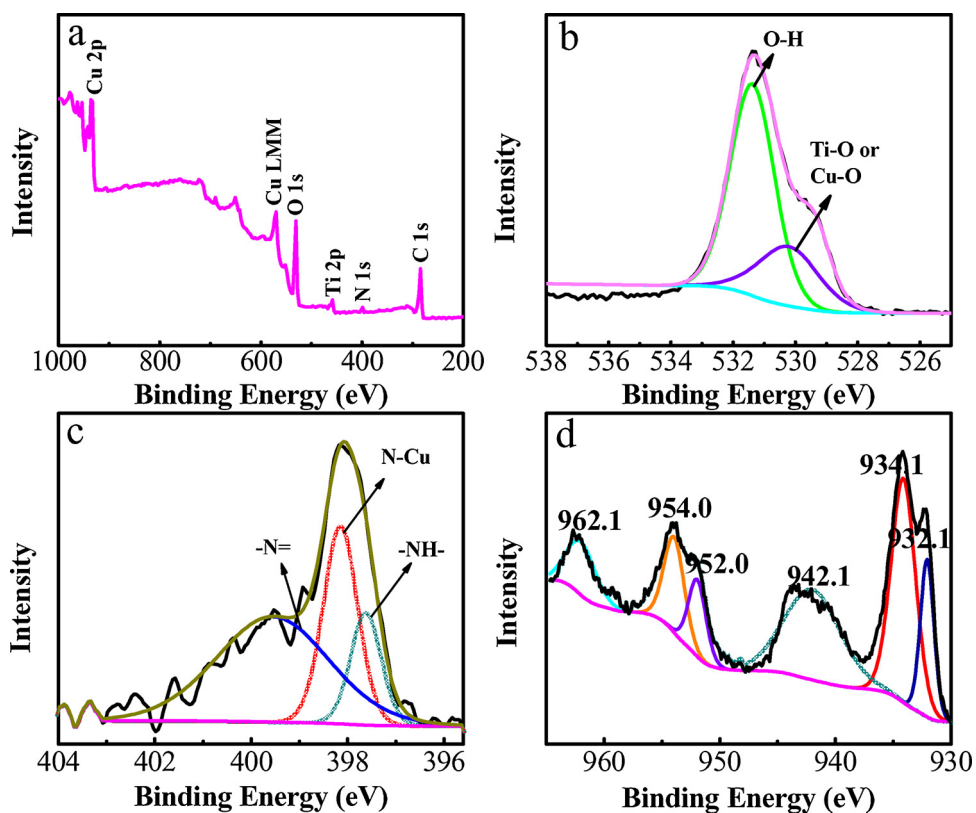


Fig. 6. Typical XPS spectra of the  $\text{TiO}_2$  MS-Cu-TCPP: survey spectrum (a), and high resolution XPS spectra of (b) O1s, (c) N1s, and (d) Cu2p.

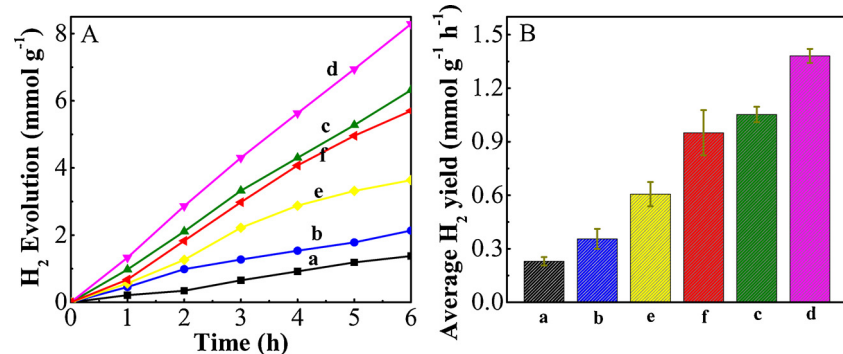
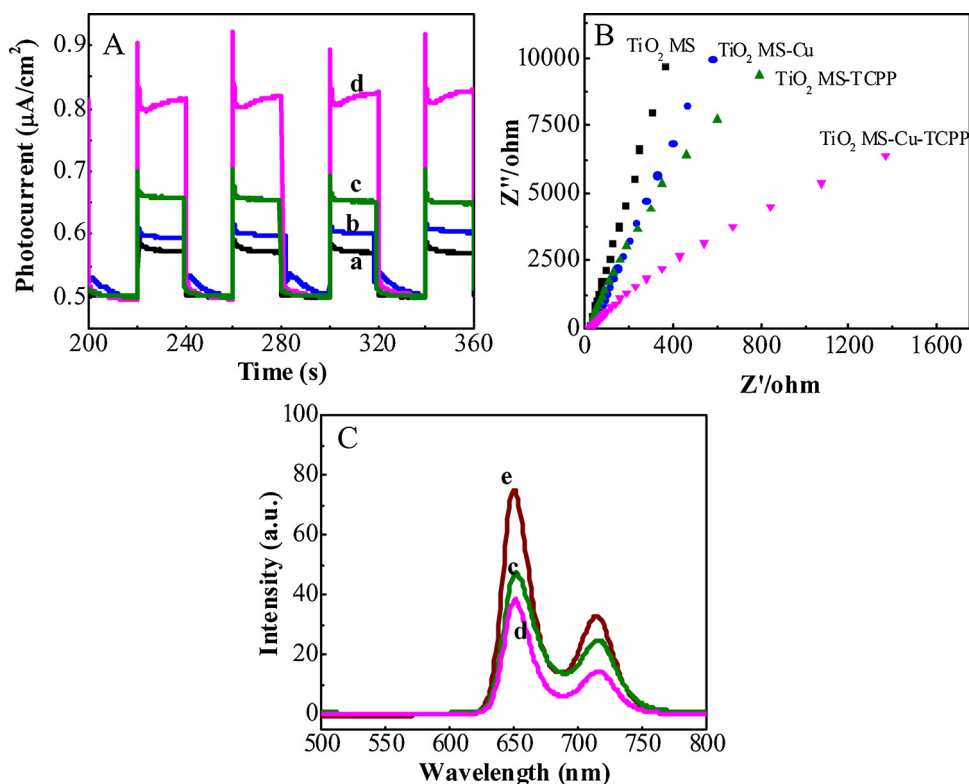


Fig. 7. (A) The dependence of  $\text{H}_2$  evolution over various photocatalysts on irradiation time. (B) The  $\text{H}_2$  evolution rates over various photocatalysts.  $\text{TiO}_2$  MS (a),  $\text{TiO}_2$  MS-Cu (b),  $\text{TiO}_2$  MS-TCPP (c),  $\text{TiO}_2$  MS-Cu-TCPP (d),  $\text{TiO}_2$  MS-TCPP-Cu (e) and  $\text{TiO}_2$  MS-Cu-TCPP (f).

at  $1701\text{ cm}^{-1}$ , the symmetric  $\text{COO}^-$  stretching vibration band at  $1600\text{ cm}^{-1}$  and  $1400\text{ cm}^{-1}$ , and the O-H stretching vibration band at  $1240\text{ cm}^{-1}$  [17], can be observed, respectively. After TCPP molecules were linked on the  $\text{TiO}_2$  MS-Cu, the bands at  $1701\text{ cm}^{-1}$  and  $1240\text{ cm}^{-1}$  are almost vanish, supporting the hydrogen bond interaction between TCPP and  $\text{TiO}_2$  MS by carboxyl groups of TCPP and hydroxyl groups of  $\text{TiO}_2$  MS. In addition, the stretching vibration band at  $964\text{ cm}^{-1}$  disappears, and a new band at  $1000\text{ cm}^{-1}$  appears. It is one of the most prominent features of the metalation of porphyrin macrocycle [18,22], which indicates that some TCPP molecules coordinate with the Cu on the  $\text{TiO}_2$  MS. The results are consistent with those in UV-vis diffuse reflectance absorption spectra (Fig. 4).

More details concerning the elemental compositions and the surface chemical states of the  $\text{TiO}_2$  MS-Cu-TCPP nano-micro hybrid were further investigated by X-ray photoelectron spectroscopy (XPS). Fig. 6a shows the representative XPS survey spectrum of the  $\text{TiO}_2$  MS-Cu-TCPP hybrid, revealing the existence of Ti, O, Cu, N and C elements within the hybrid, which are consistent with the elemental composition in the

$\text{TiO}_2$  MS-Cu-TCPP hybrid. The high resolution XPS spectra of O1s, N1s and Cu2p are measured and shown in Fig. 6b-d, respectively. In the high resolution XPS spectrum of O1s (Fig. 6b), the peak at the binding energy of ca.  $530.3\text{ eV}$  is assigned to Ti-O/Cu-O species, and the one at a higher binding energy of ca.  $531.4\text{ eV}$  indicates the presence of hydroxides/ carboxides in the hybrid [23]. In high resolution XPS spectrum of N1s (Fig. 6c), the peaks centered at  $399.6\text{ eV}$  and  $397.6\text{ eV}$  correspond to  $=\text{N}-$  and  $\text{N}-\text{H}$  of pyrrole, respectively [18]. The peak centered at  $398.1\text{ eV}$  is attributed to Cu-N [24], which indicates the coordination interaction between the Cu and TCPP macrocycle in the hybrid. In the high resolution XPS spectrum of Cu2p (Fig. 6d), two peaks centered at ca.  $932.1$  and  $952.0\text{ eV}$  are attributed to metallic Cu. Because the peaks of Cu are close to those of the  $\text{Cu}_2\text{O}$  [25],  $\text{Cu}_2\text{O}$  is probably present in the hybrid (it was not shown in XRD, also possibly due to its low crystallinity, low content, and good dispersion). The main peaks at ca.  $934.1$  and  $954.0\text{ eV}$ , along with the shakeup satellite peaks at ca.  $942.1$  and  $962.1\text{ eV}$ , indicate the existence of  $\text{Cu}^{2+}$  [26]. It is deduced that some Cu on the hybrid were oxidized to  $\text{CuO}$  due to the



**Fig. 8.** (A) Transient photocurrents; (B) Nyquist plots of electrochemical impedance spectra and (C) fluorescence spectra of various samples. (a)  $\text{TiO}_2$  MS, (b)  $\text{TiO}_2$  MS-Cu, (c)  $\text{TiO}_2$  MS-TCPP, (d)  $\text{TiO}_2$  MS-Cu-TCPP and (e) TCPP.  $\lambda_{\text{ex}} = 420 \text{ nm}$ .

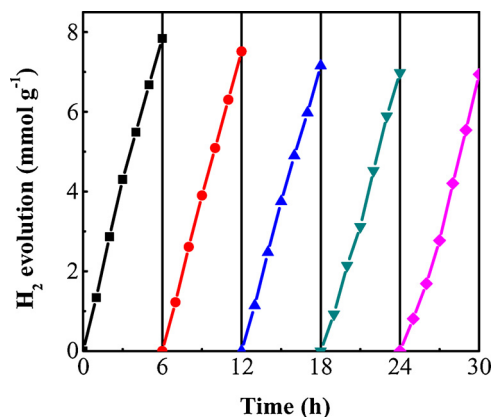


**Fig. 9.** Cycling measurements of  $\text{H}_2$  evolution over the  $\text{TiO}_2$  MS-Cu-TCPP nano-micro hybrid.

linking of TCPP on the  $\text{TiO}_2$  MS-Cu, which is consistent with the XRD result (Fig. 3c). Subsequently, there exist metallic Cu and  $\text{Cu}_2\text{O}/\text{CuO}$  in the  $\text{TiO}_2$  MS-Cu-TCPP hybrid. The influence of Cu species on the photocatalytic activity of the hybrid will be further discussed in Figs. 9 and 10.

Based on the results of Fig. 1, Figs. 4–6 and our previous reports [17,18], it is demonstrated that the  $\text{TiO}_2$  MS-Cu-TCPP nano-micro hybrid was obtained, and the combination mode of TCPP and  $\text{TiO}_2$  MS-Cu can be concluded in two ways: hydrogen bond interaction coming from carboxylic groups of TCPP with the hydroxyl groups on  $\text{TiO}_2$  (confirmed by UV-vis spectra and FTIR spectra); and coordination interaction between TCPP macrocycle and the Cu on  $\text{TiO}_2$  MS (evidenced by UV-vis spectra, FTIR spectra and XPS spectra), just like that shown in Scheme 1. The intimate contact originated from the dual interaction between  $\text{TiO}_2$  MS-Cu and TCPP is very profitable to improving electron transfer and photocatalytic activity of the products. In the absence of any other additives, the assembly of  $\text{TiO}_2$  MS-Cu and TCPP may pave a

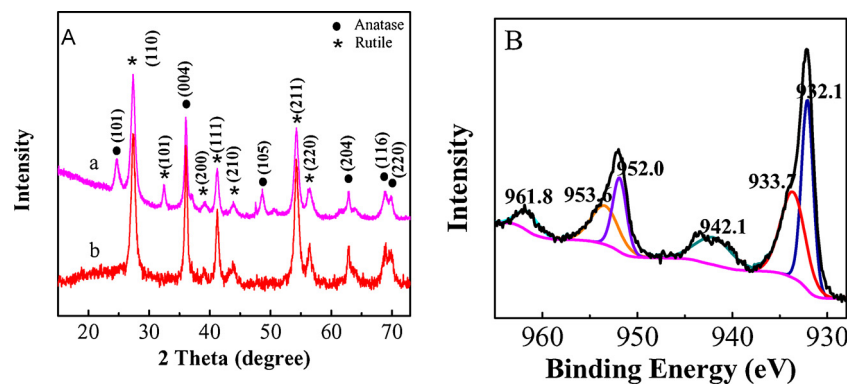


**Fig. 10.** (A) XRD patterns of the  $\text{TiO}_2$  MS-Cu-TCPP: before (a) and after (b) photocatalytic hydrogen evolution. (B) The high resolution XPS spectrum of Cu2p in the  $\text{TiO}_2$  MS-Cu-TCPP after photocatalytic hydrogen evolution.

way for the formation of a novel  $\text{TiO}_2$  hybrid by combining hydrogen bond interaction and coordination interaction.

### 3.2. Photocatalytic activity for hydrogen evolution and electron transfer mechanism

The photocatalytic activity for  $\text{H}_2$  production over the as-prepared products was evaluated by using TEOA as sacrificial agents and irradiated under a 300 W xenon lamp. It can be seen that, in Fig. 7, the activity of  $\text{TiO}_2$  MS-Cu (Fig. 7b) is higher than that of  $\text{TiO}_2$  MS (Fig. 7a), indicating of the role of cocatalyst Cu in the  $\text{TiO}_2$  MS. Furthermore, the  $\text{TiO}_2$  MS-Cu-TCPP nano-micro hybrid exhibits significantly enhanced photocatalytic activities as compared to those of the  $\text{TiO}_2$  MS-TCPP-Cu,  $\text{TiO}_2$  MS-Cu-CuTCPP,  $\text{TiO}_2$  MS-TCPP,  $\text{TiO}_2$  MS-Cu and  $\text{TiO}_2$  MS. Its  $\text{H}_2$  release rate is enhanced for more than 6 times with respect to the pure  $\text{TiO}_2$  MS, resulting from the strong interaction and efficient electron transfer in the hybrid with the Cu as the linker (further evidenced by the followed Fig. 8). Moreover, it is found that the increased amount of hydrogen is different after introducing Cu in the  $\text{TiO}_2$  MS and in the  $\text{TiO}_2$  MS-TCPP, respectively. It shows larger enhancement when Cu is introduced into  $\text{TiO}_2$  MS-TCPP (about 3.8 times higher in  $\text{TiO}_2$  MS-Cu-TCPP, and about 2.9 times higher in  $\text{TiO}_2$  MS-TCPP-Cu than that introduced in the  $\text{TiO}_2$  MS). Moreover, the activity of the  $\text{TiO}_2$  MS-Cu-TCPP is 2.3 times higher than that of the  $\text{TiO}_2$  MS-TCPP-Cu, and 1.45 times higher than that of the  $\text{TiO}_2$  MS-Cu-CuTCPP. Combined with the results in Figs. 3–5, it is demonstrated the important role of Cu in the hybrid as the bridging agent between  $\text{TiO}_2$  MS and TCPP, and the synergistic effect of Cu NPs in the  $\text{TiO}_2$  MS-Cu-TCPP hybrid, which can facilitate the electron transfer from TCPP to  $\text{TiO}_2$  MS. Additionally, the coordination ratio of Cu to TCPP is 1: 1, while the molar ratio of Cu to TCPP in the hybrid is about 1: 0.001. Therefore, only a small amount of Cu covered with TCPP, which is also confirmed by HRTEM of the  $\text{TiO}_2$  MS-Cu-TCPP (Fig. 1f, the plane of Cu species can be clearly observed). The rest Cu can act as the cocatalyst, namely, the active sites where  $\text{H}_2$  was evolved. Moreover, the photocatalytic activity of the  $\text{TiO}_2$  MS-Cu-TCPP (Fig. 7d) is higher than that of the  $\text{TiO}_2$  MS-Cu-CuTCPP (Fig. 7f). In addition, visible light absorption of the  $\text{TiO}_2$  MS-Cu-CuTCPP and  $\text{TiO}_2$  MS-Cu-TCPP is similar. Therefore, the higher activity in the  $\text{TiO}_2$  MS-Cu-TCPP is mainly attributed to the coordination of TCPP macrocycle and the Cu species on the  $\text{TiO}_2$  MS, and the synergistic effect of Cu NPs in the  $\text{TiO}_2$  MS-Cu-TCPP hybrid, which can facilitate the electron transfer from TCPP to  $\text{TiO}_2$  MS. These are vital to enhance the photocatalytic activity of a photocatalyst.

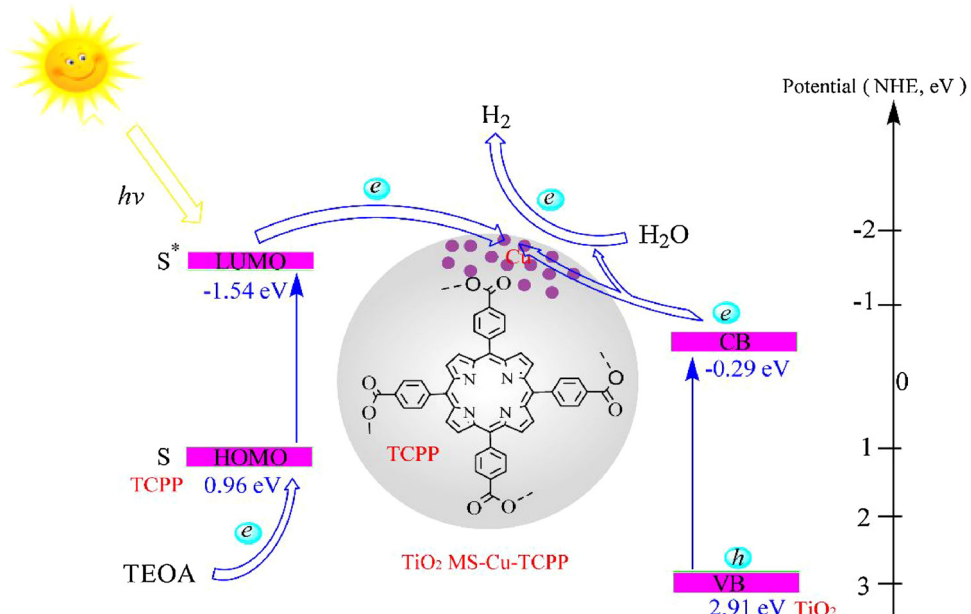
In order to explore the reason for the enhanced photocatalytic activity in the  $\text{TiO}_2$  MS-Cu-TCPP nano-micro hybrid, electron transfer, interfacial resistance and fluorescence for the samples are investigated. The separation of photogenerated charge is important for a photocatalyst. To prove the efficient separation of photogenerated charge carriers in the synthesized  $\text{TiO}_2$  MS-Cu-TCPP hybrid, photocurrent measurements of the samples were carried out in several on-off intermittent irradiation cycles and the results are shown in Fig. 8A. It reveals that photocurrent intensity enhances when the light is on, and it quickly decreases when the light is off. It is demonstrated that the samples are photosensitive. The photocurrent of all samples is in the order of  $\text{TiO}_2$  MS-Cu-TCPP >  $\text{TiO}_2$  MS-TCPP >  $\text{TiO}_2$  MS-Cu >  $\text{TiO}_2$  MS. Obviously, the introduction of TCPP can greatly improve the photocurrent of  $\text{TiO}_2$  MS. Furthermore, the  $\text{TiO}_2$  MS-Cu-TCPP hybrid shows about 2 times higher photocurrent response than that of the  $\text{TiO}_2$  MS-TCPP. The increased photocurrent response for the  $\text{TiO}_2$  MS-Cu-TCPP suggests that photogenerated electron-hole pairs are highly separated and recombination rate is decreased under light irradiation. Charge carriers transfer process over the hybrid could be attributed to strong interaction between TCPP and Cu, and also confirms the significant role of Cu in the  $\text{TiO}_2$  MS-Cu-TCPP hybrid. Consequently, protons can capture more electrons to form  $\text{H}_2$ . Moreover, the photocurrent responses are highly reproducible and remain stable for several on-off cycles,

indicating that the nano-micro hybrid can effectively resist photo-corrosion. In addition, the photocurrent of the  $\text{TiO}_2$  MS-Cu is higher than that of the  $\text{TiO}_2$  MS, which further supports the dual roles of Cu in the  $\text{TiO}_2$  MS-Cu-TCPP hybrid. It is consistent with the results of Fig. 7.

Besides photocurrent response, the charge carrier migration in the  $\text{TiO}_2$  MS-Cu-TCPP nano-micro hybrid can be studied by electrochemical impedance spectroscopy. As is shown in Fig. 8B, the diameters of the semicircles at high frequencies for various samples are distinctly different. According to the diameter of the semicircles, the interfacial resistance of the samples is in the order of  $\text{TiO}_2$  MS >  $\text{TiO}_2$  MS-Cu >  $\text{TiO}_2$  MS-TCPP >  $\text{TiO}_2$  MS-Cu-TCPP. It is indicated that the introduction of Cu and/or TCPP can efficiently decrease the interfacial resistance of the  $\text{TiO}_2$  MS. In addition, electrochemical impedance of the  $\text{TiO}_2$  MS-Cu-TCPP hybrid is lower than that of the  $\text{TiO}_2$  MS-TCPP. It shows the important role of Cu in the hybrid, which could improve the contact and the interaction between  $\text{TiO}_2$  MS and TCPP (Fig. 1c), which is profitable to improving the electron transfer and photocatalytic activity of the  $\text{TiO}_2$  MS-Cu-TCPP nano-micro hybrid. The result supports the fact that the introduction of Cu in the  $\text{TiO}_2$  MS-TCPP can modify the interaction between  $\text{TiO}_2$  MS and TCPP, and has a positive influence on the photocatalytic activity of the  $\text{TiO}_2$  MS-TCPP. The result is consistent with that in Fig. 8A.

Furthermore, fluorescence measurements can provide the information on the photogenerated electron-hole separation. The fluorescence spectra of samples are measured and shown in Fig. 8C. Two emission peaks located at 650 nm and 714 nm are observed for the TCPP. After introducing  $\text{TiO}_2$  MS and  $\text{TiO}_2$  MS-Cu into the TCPP solution, respectively, the fluorescence spectra are similar to that of the TCPP except the quenched emission peaks. It suggests fast photo-induced electron transfer and low charge recombination. Moreover, the weak emission bands indicate that most of the surface states are passivated, making the electrons available for photocatalytic  $\text{H}_2$  evolution [27]. Obviously, the recombination of the electrons and holes can be efficiently inhibited, deduced from the decreased fluorescence. It confirms that the interaction between TCPP and  $\text{TiO}_2$  MS is strengthened with Cu as the linker. The result is consistent with those in Fig. 8A and B. Therefore, more photogenerated electrons become involved into reducing  $\text{H}^+$  to  $\text{H}_2$ , which reduces recombination.

Reusability of a photocatalyst is one of the most important factors in catalysis research as well as for practical application. Therefore, recyclability experiments were conducted under a 300 W xenon lamp in order to estimate the stability of the prepared  $\text{TiO}_2$  MS-Cu-TCPP nano-micro hybrid. The optimized  $\text{TiO}_2$  MS-Cu-TCPP was tested by five consecutive photocatalytic activity experiments, and each reaction was performed for 6 h of irradiation time, as shown in Fig. 9. It can be seen that, there is no obvious loss of photocatalytic activity of hydrogen production after 5 cycles using the  $\text{TiO}_2$  MS-Cu-TCPP as the photocatalyst. In the second recycle, the amount of hydrogen evolution over the nano-micro hybrid is slightly decreased, and the amount of hydrogen evolution is hardly changed from the third time. As shown in Fig. 10A, after the illumination, the main peaks corresponding to anatase  $\text{TiO}_2$  and rutile  $\text{TiO}_2$  are same as those in the as-prepared  $\text{TiO}_2$  MS-Cu-TCPP except the peaks corresponding to (101) plane and (105) plane of  $\text{TiO}_2$ , which could be caused by the redistribution of Cu and TCPP on  $\text{TiO}_2$  MS. In addition, after the illumination, the peaks corresponding to  $\text{Cu}^{2+}$  decrease, and shift towards low binding energy, which indicate that the  $\text{Cu}^{2+}$  on the surface of the catalyst can be partially reduced by the  $\text{H}_2$  evolved. Referenced to the literature [28], the transformation of  $\text{Cu}^{2+}$  to the other Cu species ( $\text{Cu}/\text{Cu}^+$ ) have positive not negative effect on the activity of  $\text{TiO}_2$  MS-Cu-TCPP hybrid. Therefore, the slightly decreased activity in the third time is attributed to the redistribution of Cu and TCPP in the  $\text{TiO}_2$  MS, or a certain amount of THPP molecules taken off from the surface of the  $\text{TiO}_2$  MS-Cu under the weak basic condition [29] (Measurement of photocatalytic activity was performed in TEOA aqueous solution, and the pH value was about 8–9). Due to the partial loss of the TCPP on the  $\text{TiO}_2$  MS-Cu



**Scheme 2.** Schematic representation of the electron transfer in the  $\text{TiO}_2$  MS-Cu-TCPP nano-micro hybrid under light irradiation.

TCPP, the pH value of the solution is slightly decreased. When the pH value is close to neutral, the TCPP molecules, especially those linked strongly on the  $\text{TiO}_2$  MS-Cu-TCPP, are not taken off any more. Therefore, the amount of hydrogen evolution is hardly changed. The result suggests that the photocatalytic activity over the  $\text{TiO}_2$  MS-Cu-TCPP hybrid is relatively stable.

In order to explore the enhanced and stable photocatalytic activity over the  $\text{TiO}_2$  MS-Cu-TCPP hybrid, a proposed mechanism is schematically illustrated in **Scheme 2** (HUMO and LUMO values of TCPP, and CB and VB of  $\text{TiO}_2$  were obtained from the references [30,31], respectively). According to the semiconductor photocatalytic theory, the amount of excited electrons in the interface of water and photocatalyst is vital to the photocatalytic activity [32]. In the  $\text{TiO}_2$  MS-Cu-TCPP hybrid, excited electrons can be produced by  $\text{TiO}_2$  MS and TCPP after irradiation, mainly coming from the TCPP. Since the Fermi level of metal Cu is relatively low comparing to those of  $\text{TiO}_2$  and TCPP [33], which is conducive to the photoinduced electrons transfer from  $\text{TiO}_2$  MS and TCPP to the Cu. Therefore, the Cu in the  $\text{TiO}_2$  MS-Cu-TCPP can act as the transfer passageway of the electrons, which make the recombination of electrons and holes be efficiently avoided. Besides, it can act as the cocatalyst to provide active sites for photocatalytic hydrogen production. Hence, the Cu in the  $\text{TiO}_2$  MS-Cu-TCPP hybrid acts as key roles in enhancing the photocatalytic activity of  $\text{H}_2$  production. Overall, the constructed  $\text{TiO}_2$  MS-Cu-TCPP hybrid photocatalyst can bring the synergistic effect such as enhanced light absorption, improved interfacial charge transfer, and increased reaction centers, which consequently make a significant enhancement on its photocatalytic performance. The photo-produced electrons produced are captured by water molecules, and then the water molecules are reduced into  $\text{H}_2$  (**Fig. 7**), and the holes are consumed by the TEOA.

#### 4. Conclusions

With Cu NPs as the bridging agent, a novel  $\text{TiO}_2$  MS-Cu-TCPP nano-micro hybrid was prepared by means of hydrogen bond interaction and coordination interaction. It was found that the Cu had an important influence on the assembly of TCPP on the  $\text{TiO}_2$  MS. Moreover, the Cu in the  $\text{TiO}_2$  MS-Cu-TCPP can act as the passageway of the electron transfer, which was conducive to the photoinduced electrons transfer and electrons/holes separation. Besides, it can act as the cocatalyst to provide active sites for photocatalytic hydrogen production. Hence, the

constructed  $\text{TiO}_2$  MS-Cu-TCPP hybrid photocatalysts can bring synergistic effects such as enhanced light absorption, improved interfacial charge transfer, and increased reaction centers. Subsequently, the hybrid showed about 6 times higher activity than that of the pure  $\text{TiO}_2$  MS under the same conditions. It is expected that current work can provide a facile strategy via interface and microstructure modulation for exploring excellent photocatalysts to be used in photocatalytic clean energy production.

#### Acknowledgements

This work was financially supported by the National Natural Science Foundation of China (No. 21771125, 21301118 and 21305092) and Innovation Fund of China Petroleum Science & Technology (No. 2107D-5007-0207).

#### References

- [1] Y. Ma, X.L. Wang, Y.S. Jia, X.B. Chen, H.X. Han, C. Li, Titanium dioxide-based nanomaterials for photocatalytic fuel generations, *Chem. Rev.* 114 (2014) 9987–10043.
- [2] M. Gopannagari, D.P. Kumar, D.A. Reddy, S. Hong, M.I. Song, T.K. Kim, In situ preparation of few-layered  $\text{WS}_2$  nanosheets and exfoliation into bilayers on  $\text{GdS}$  nanorods for ultrafast charge carrier migrations toward enhanced photocatalytic hydrogen production, *J. Catal.* 351 (2017) 153–160.
- [3] Q. Wang, T. Hisatomi, Q.X. Jia, H. Tokudome, M. Zhong, C.Z. Wang, Z.H. Pan, T. Takata, M. Nakabayashi, N. Shibata, Y.B. Li, I.D. Sharp, A. Kudo, T. Yamada, K. Domen, Scalable water splitting on particulate photocatalyst sheets with a solar-to-hydrogen energy conversion efficiency exceeding 1%, *Nat. Mater.* 15 (2016) 611–615.
- [4] H.L. Hou, L. Wang, F.M. Gao, G.D. Wei, J.J. Zheng, B. Tang, W.Y. Yang, Hierarchically porous  $\text{TiO}_2/\text{SiO}_2$  fibers with enhanced photocatalytic activity, *RSC Adv.* 4 (2014) 19939–19944.
- [5] M.Z. Ge, C.Y. Cao, J.Y. Huang, S.H. Li, Z. Chen, K.Q. Zhang, S.S.A. Deyabd, Y.K. Lai, A review of one-dimensional  $\text{TiO}_2$  nanostructured materials for environmental and energy applications, *J. Mater. Chem. A* 4 (2016) 6772–6801.
- [6] F.Y. Xu, J.J. Zhang, B.C. Zhu, J.G. Yu, J.S. Xu,  $\text{CuInS}_2$  sensitized  $\text{TiO}_2$  hybrid nanofibers for improved photocatalytic  $\text{CO}_2$  reduction, *Appl. Catal. B: Environ.* 230 (2018) 194–202.
- [7] W. Shao, F. Gu, C.Z. Li, M.K. Lu, Interfacial confined formation of mesoporous spherical  $\text{TiO}_2$  nanostructures with improved photoelectric conversion efficiency, *Inorg. Chem.* 49 (2010) 5453–5459.
- [8] J.G. Hou, C. Yang, Z. Wang, S.Q. Jiao, H.M. Zhu,  $\text{Bi}_2\text{O}_3$  quantum dots decorated anatase  $\text{TiO}_2$  nanocrystals with exposed {001} facets on graphene sheets for enhanced visible-light photocatalytic performance, *Appl. Catal. B: Environ.* 129 (2013) 333–341.
- [9] M.M. Islam, T. Bredow, Rutile band-gap states induced by doping with manganese

in various oxidation states, *J. Phys. Chem. C* 119 (2015) 5534–5541.

[10] S. Meia, J.P. Gao, Y. Zhang, J.B. Yang, Y.L. Wu, X.X. Wang, R.R. Zhao, X.G. Zhai, C.Y. Hao, R.X. Lia, Yan J, Enhanced visible light photocatalytic hydrogen evolution over porphyrin hybridized graphitic carbon nitride, *J. Colloid Interface Sci.* 506 (2017) 58–65.

[11] R.Y. Ge, X.Q. Li, S.Z. Kang, L.X. Qin, G.D. Li, Highly efficient graphene oxide/porphyrin photocatalysts for hydrogen evolution and the interfacial electron transfer, *Appl. Catal. B: Environ.* 187 (2016) 67–74.

[12] S. Murphy, C. Saurel, A. Morrissey, J. Tobin, M. Oelgemöller, K. Nolan, Photocatalytic activity of a porphyrin/TiO<sub>2</sub> composite in the degradation of pharmaceuticals, *Appl. Catal. B: Environ.* 119 (2012) 156–165.

[13] G. Landrou, A.A. Panagiotopoulos, K. Ladomenou, A.G. Coutsolelos, Photochemical hydrogen evolution using Sn-porphyrin as photosensitizer and a series of cobaloximes as catalysts, *J. Porphyrins Phthalocyanines* 20 (2016) 534–541.

[14] R. Su, R. Tiruvalam, A.J. Logsdail, Q. He, C.A. Downing, M.T. Jensen, N. Dimitratos, L. Kesavan, P.P. Wells, R. Bechstein, H.H. Jensen, S. Wendt, R.A. Catlow, C.J. Kiely, G.J. Hutchings, F. Besenbacher, Designing titania-supported Au-Pd nanoparticles for efficient photocatalytic hydrogen production, *ACS Nano* 8 (2014) 3490–3497.

[15] E.P. Melián, M.N. Suárez, T. Jardiel, J.M.D. Rodríguez, A.C. Caballero, J. Arana, D.G. Calatayud, O.G. Díaz, Influence of nickel in the hydrogen production activity of TiO<sub>2</sub>, *Appl. Catal. B: Environ.* 152 (2014) 192–201.

[16] M.R. Pai, A.M. Banerjee, S.A. Rawool, A. Singh, C. Nayak, S.H. Ehrman, A.K. Tripathi, S.R. Bharadwaj, A comprehensive study on sunlight driven photocatalytic hydrogen generation using low cost nanocrystalline Cu-Ti oxides, *Sol. Energy Mater. Sol. Cells* 154 (2016) 104–120.

[17] B. Zhuang, X.Q. Li, S.Z. Kang, L.X. Qin, G.D. Li, Assembly and electron transfer mechanisms on visible light responsive 5,10,15,20-meso-tetra(4-carboxyphenyl) porphyrin/cuprous oxide composite for photocatalytic hydrogen production, *Appl. Catal. A* 533 (2017) 81–89.

[18] R.Y. Ge, X.Q. Li, B. Zhuang, S.Z. Kang, L.X. Qin, G.D. Li, Assembly mechanism and photoproduced electron transfer for a novel cubic Cu<sub>2</sub>O/tetrakis(4-hydroxyphenyl) porphyrin hybrid with visible photocatalytic activity for hydrogen evolution, *Appl. Catal. B: Environ.* 211 (2017) 296–304.

[19] L. Tu, H. Pan, H.X. Xie, A. Yu, M.G. Xu, Q.L. Chai, Y.M. Cui, X.F. Zhou, Study on the fabrication and photovoltaic property of TiO<sub>2</sub> mesoporous microspheres, *Solid State Sci.* 14 (2012) 616–621.

[20] W.L. Zhen, W.J. Jiao, Y.Q. Wu, H.W. Jing, G.X. Lu, The role of a metallic copper interlayer during visible photocatalytic hydrogen generation over a Cu/Cu<sub>2</sub>O/Cu/TiO<sub>2</sub> catalyst, *Catal. Sci. Technol.* 7 (2017) 5028–5037.

[21] W. Zhang, C. Wang, X. Liu, J. Li, Enhanced photocatalytic activity in porphyrin sensitized TiO<sub>2</sub> nanorods, *J. Mater. Res.* 32 (2017) 2773–2780.

[22] D.D. La, H.P.N. Thi, Y.S. Kim, A. Ranaware, S.V. Bhosale, Facile fabrication of Cu (II)-porphyrin MOF thin films from tetrakis (4-carboxyphenyl) porphyrin and Cu (OH)<sub>2</sub> nanoneedle array, *Appl. Surf. Sci.* 424 (2017) 145–150.

[23] S.S. Lee, H.W. Bai, Z.Y. Liu, D.D. Sun, Novel-structured electrospun TiO<sub>2</sub>/CuO composite nanofibers for high efficient photocatalytic cogeneration of clean water and energy from dye wastewater, *Water Res.* 47 (2013) 4059–4073.

[24] Y.Y. Liu, Y.M. Yang, Q.L. Sun, Z.Y. Wang, B.B. Huang, Y. Dai, X.Y. Qin, X.Y. Zhang, Chemical adsorption enhanced CO<sub>2</sub> capture and photoreduction over a copper porphyrin based metal organic framework, *ACS Appl. Mater. Interfaces* 5 (2013) 7654–7658.

[25] J. Xing, Z.P. Chen, F.Y. Xiao, X.Y. Ma, C.Z. Wen, Z. Li, H.G. Yang, Cu-Cu<sub>2</sub>O-TiO<sub>2</sub> nanojunction systems with an unusual electron-hole transportation pathway and enhanced photocatalytic properties, *Chem. Asian J.* 8 (2013) 1265–1270.

[26] H.L. Hou, M.H. Shang, F.M. Gao, L. Wang, Q. Liu, J.J. Zheng, Z.B. Yang, W.Y. Yang, Highly efficient photocatalytic hydrogen evolution in ternary hybrid TiO<sub>2</sub>/CuO/Cu thoroughly mesoporous nanofibers, *ACS Appl. Mater. Interfaces* 8 (2016) 20128–20137.

[27] W.L. Zhen, W.J. Jiao, Y.Q. Wu, H.W. Jing, G.X. Lu, The role of a metallic copper interlayer during visible photocatalytic hydrogen generation over a Cu/Cu<sub>2</sub>O/Cu/TiO<sub>2</sub> catalyst, *Catal. Sci. Technol.* 7 (2017) 5028–5037.

[28] D.A. Reddy, J. Choi, S. Lee, Y. Kim, S. Hong, D.P. Kumar, T.K. Kim, Hierarchical dandelion-flower-like cobalt-phosphide modified CdS/reduced graphene oxide-MoS<sub>2</sub> nanocomposites as a noble-metal-free catalyst for efficient hydrogen evolution from water, *Catal. Sci. Technol.* 6 (2016) 6197–6206.

[29] Y.J. Yuan, J.R. Tu, Z.J. Ye, H.W. Lu, Z.G. Ji, B. Hu, Y.H. Li, D.P. Cao, Z.T. Yu, Z.G. Zou, Visible – light – driven hydrogen production from water in a noble-metal-free system catalyzed by zinc porphyrin sensitized MoS<sub>2</sub>/ZnO, *Dyes Pigments* 123 (2015) 285–292.

[30] S.K. Mei, J.P. Gao, Y. Zhang, J.B. Yang, Y.L. Wu, X.X. Wang, R.R. Zhao, X.G. Zhai, C.Y. Hao, R.X. Li, J. Yan, Enhanced visible light photocatalytic hydrogen evolution over porphyrin hybridized graphitic carbon nitride, *J. Colloid Interface Sci.* 506 (2017) 58–65.

[31] N.L. Reddy, S. Emin, V.D. Kumari, S.M. Venkatakrishnan, CuO quantum dots decorated TiO<sub>2</sub> nanocomposite photocatalyst for stable hydrogen generation, *Ind. Eng. Chem. Res.* 57 (2018) 568–577.

[32] X.B. Chen, S.H. Shen, L.J. Guo, S.S. Mao, Semiconductor-based photocatalytic hydrogen generation, *Chem. Rev.* 110 (2010) 6503–6570.

[33] M.A. Mamun, Y. Kusumoto, B. Ahmmad, M.S. Islam, Photocatalytic cancer (HeLa) cell-killing enhanced with Cu-TiO<sub>2</sub> nanocomposite, *Top. Catal.* 53 (2010) 571–577.